ISSN 0036-0236, Russian Journal of Inorganic Chemistry, 2022, Vol. 67, No. 2, pp. 123–130. © Pleiades Publishing, Ltd., 2022.
Russian Text © The Author(s), 2022, published in Zhurnal Neorganicheskoi Khimii, 2022, Vol. 67, No. 2, pp. 139–147.

Synthesis of Highly Dispersed Powder Ceramic Composition Si_3N_4–SiC by Combustion of Components in the Si–C–NaN_3–NH_4F System

A. P. Amosov[a, *], G. S. Belova[a], Yu. V. Titova[a], and D. A. Maidan[a]

[a] *Samara State Technical University, Samara, 443100 Russia*
**e-mail: egundor@yandex.ru*

Received August 7, 2021; revised August 26, 2021; accepted August 31, 2021

Abstract—The possibility of synthesizing a highly dispersed powder nitride-carbide composition Si_3N_4–SiC by combustion of a mixture of sodium azide (NaN_3) with elemental powders of silicon (Si) and soot (C) and an activating addition of ammonium fluoride (NH_4F) in a nitrogen atmosphere has been investigated. The combustion parameters, chemical and phase composition, morphology, and particle sizes of the synthesized products have been determined. It is shown that, after water washing, the powder combustion product consists of silicon nitride of two modifications (α-Si_3N_4 and β-Si_3N_4) with a predominant content of α-Si_3N_4, silicon carbide (β-SiC) in an amount from 1.6 to 41.8%, and an insignificant amount of free silicon (Si). In most cases, the obtained nitride-carbide composition Si_3N_4–SiC is a mixture of submicron (0.1–0.5 μm) fibers and equiaxed particles, promising for low-temperature sintering of the corresponding structural composite ceramic materials with enhanced mechanical properties.

Keywords: sodium azide, ammonium fluoride, combustion, synthesis, Si_3N_4–SiC
DOI: 10.1134/S0036023622020024

INTRODUCTION

Silicon nitride Si_3N_4 and silicon carbide SiC are refractory compounds used for the manufacture of the corresponding non-oxide ceramic materials, both structural (due to high melting points, hardness, wear resistance, heat resistance, and chemical stability) and functional purpose (due to electrical and catalytic properties) [1–5]. The Si_3N_4 dielectric is used as an insulator in microelectronics, as well as a storage medium in flash memory devices, whereas the SiC semiconductor is used in high-power high-temperature transistor devices and LEDs, as well as electric heaters. Silicon carbide is used as a catalyst in the oxidation of hydrocarbons, and silicon nitride is used as a catalyst carrier. However, these ceramic materials differ markedly in some characteristics. The specific values of the characteristics strongly depend on the methods of obtaining ceramics; we use the averaged values of the characteristics determined mainly at room temperature. For example, Si_3N_4 ceramics are not as brittle as SiC, they exhibit high fracture toughness (on average 5.3 MPa $m^{1/2}$) and good flexural strength (at the level of 750 MPa), but it is characterized by low resistance to oxidation at high temperatures (an increase in the mass of 1.2 mg/cm^3 at 1573 K for 100 h) [1, 4]. SiC ceramics, on the other hand, demonstrates high resistance to wear, creep, and oxidation at high temperatures (an increase in mass of 0.02 mg/cm^3 under the same conditions), but low values of flexural strength (450 MPa) and fracture toughness (2.8 MPa $m^{1/2}$). Silicon carbide is the most important component (20–65 vol %) of ultrahigh-temperature ceramic materials to achieve their maximum oxidation resistance [6–9]. The results of a large number of studies show that the combination of silicon nitride and silicon carbide in the Si_3N_4–SiC composite material makes it possible to use the advantages of each of these single-phase ceramics and obtain composite ceramics with significantly improved properties, primarily for high-temperature applications [4, 5, 10–15]. The introduction of only 5 vol % SiC into a Si_3N_4 matrix makes it possible to obtain a composite with an increased fracture toughness of 6.5 MPa $m^{1/2}$ by spark plasma sintering [15]. The Si_3N_4–20 vol % SiC composite made by hot isostatic pressing has a fracture toughness of 9.5 MPa $m^{1/2}$ at a temperature of 1673 K compared to 5.3 MPa $m^{1/2}$ for single-phase ceramic Si_3N_4 and is considered a promising material for gas turbine engines [13]. This conclusion is confirmed by the results of later studies, according to which hot-pressed Si_3N_4–(20–30 vol %) SiC nanocomposites have a flexural strength of up to 1500 MPa instead of 850 MPa for conventional Si_3N_4 ceramics and retain high strength up to 1673 K instead of 1473 K for Si_3N_4

ceramics [5]. Increasing the SiC content to 40 wt % in a hot-pressed Si_3N_4–SiC composite leads to an increase in fracture toughness to a level of 10.5–12.5 MPa $m^{1/2}$ [10]. Composite ceramics Si_3N_4–SiC has great potential for its further development and application by improving the composition, structure, and properties, developing new methods of obtaining and reducing the cost of production [16, 17].

It is known that the higher the content of the α-Si_3N_4 modification in the initial silicon nitride powder, the higher the strength properties of Si_3N_4 ceramics due to the $\alpha \rightarrow \beta$-Si_3N_4 transition during sintering of materials; however, not all methods of obtaining silicon nitride powder manage to achieve a high content of its α-modification [1]. All properties of composite ceramics, including mechanical ones, can change quite significantly with an increase in the dispersion of the composite components, when passing from micron-sized particles to highly dispersed submicron (0.1–1 μm) and nanoscale (<0.1 μm = 100 nm) particles. Thus, special attention has been paid to the development of nanostructured ceramic composites [5, 12, 16, 17]. Most ceramic composites are obtained by powder technology, including mechanical mixing and grinding of the previously obtained ceramic powders of components, followed by compaction by various methods, for example, hot pressing. However, highly dispersed powders, especially nanopowders, are prone to the formation of agglomerates during their production, which prevents homogeneous mixing of powders of various components and forces us to solve the problem of deagglomeration of nanopowders [18]. Therefore, in the case of highly dispersed powders, chemical methods of direct synthesis of ceramic powders from a mixture of initial reagents are preferable rather than mechanical mixing methods [5, 16]. Submicron and nanopowder Si_3N_4–SiC compositions can be synthesized by various chemical methods, including coating Si_3N_4 particles with highly dispersed carbon as a result of methane pyrolysis [19], pyrolysis of an organic silicon-containing precursor [20], carbothermal reduction of silicon dioxide in the presence of nitrogen gas [21], gas-phase reactions [22], and plasma-chemical synthesis [23]. The listed chemical methods are characterized by high energy consumption due to the need for heating to high temperatures and the use of long exposures, the use of expensive equipment. The use of the self-propagating high-temperature synthesis (SHS) method, also known as combustion synthesis, which is characterized by low energy consumption, manufacturability, and the ability to obtain various ceramic powders, including nanopowders, from inexpensive starting components [24–26] is of undoubted interest.

The purpose of this work is to study the possibility of using the SHS method using sodium azide NaN_3 as a nitriding reagent and an activating additive of the NH_4F halide salt to obtain a highly dispersed composition of Si_3N_4–SiC powders with different phase ratios.

ANALYTICAL REVIEW

The first studies on the use of combustion for the synthesis of powder compositions Si_3N_4–SiC are based on the combustion of mixtures of powders of silicon and technical carbon (soot) in gaseous nitrogen at a pressure from 1 to 10 MPa [27–29]. The use of gaseous nitrogen as a nitriding reagent first led to the synthesis of silicon nitride with high heat release, accompanied by partial decomposition of Si_3N_4 and subsequent synthesis of silicon carbide. A mixture of Si + C powders was burned both in pure form and with the use of powder additives Si_3N_4 or fluoroplastic $(C_2F_4)_n$, which made it possible to obtain Si_3N_4–SiC compositions with different ratios of micron-sized silicon nitride and silicon carbide with a small fraction of α-Si_3N_4, sometimes with small impurities of unreacted silicon.

The use of the azide SHS method based on the use of sodium azide NaN_3 powder (instead of gaseous nitrogen) as a nitriding reagent and activating additives of gasifying halide salts made it possible to noticeably increase the fraction of α-Si_3N_4 and reduce the particle size of the Si_3N_4–SiC composition [24, 30–33]. The reaction for obtaining Si_3N_4–SiC is as follows:

$$\begin{aligned} &14Si + 6NaN_3 + (NH_4)_2SiF_6 + yC \\ &= ((15 - y)/3)Si_3N_4 + ySiC + 6NaF \\ &\quad + (2y/3)N_2 + 4H_2, \end{aligned} \tag{1}$$

where the content of carbon black was 5 or 15 moles [32]. The combustion temperature of the reagents of system (1) reached 1850°C at $y = 5$ and 1650°C at $y = 15$. In the case of $y = 5$, the cooled combustion product consisted of β-Si_3N_4, α-Si_3N_4, NaF and Si, and in the case of $y = 15$, the combustion products included α-Si_3N_4, SiC, NaF, and Si. X-ray powder diffraction showed that at $y = 5$ the content of β-Si_3N_4 prevails over the content of α-Si_3N_4, silicon carbide was not detected. At $y = 15$, on the contrary, silicon carbide is present, while β-Si_3N_4 is not found. A noticeable amount of unreacted silicon remained in the washed combustion product. Silicon carbide is an equiaxed particle with an average size of $d_{0.5} = 100$ nm, silicon nitride is a fiber with a diameter of 100–200 nm.

The use of another additive (NH_4F halide salt) in a much larger amount leads to the production of cubic tantalum nitride nanoparticles by the azide SHS method according to the reaction:

$$\begin{aligned} &K_2TaF_7 + (5 + k)NaN_3 + kNH_4F \\ &= TaN + (5 + k)NaF + 2KF + (7 + 2k)N_2 + 2kH_2, \end{aligned} \tag{2}$$

where integers k from 0 to 5 are the number of moles of the NH_4F halogen salt [34, 35]. Pure cubic TaN with d = 5–10 nm was synthesized at a content of 4 and 5 moles of NH_4F and a nitrogen pressure of 2 MPa in the combustion mode at temperatures from 850 to 950°C. The role of the NH_4F halide salt is explained by a decrease in the combustion temperature and the formation of active gaseous decomposition products. Based on the effective use of the NH_4F activating additive, it was concluded that the developed approach can be the basis for a simple and economical method for the industrial production of cubic tantalum nitride nanopowder [34].

EXPERIMENTAL

For the synthesis of target compositions Si_3N_4–SiC with a molar ratio of phases from 1 : 4 to 4 : 1, the following equations of chemical reactions were used:

$$\begin{aligned}&4Si + C + NaN_3 + NH_4F \\ &= Si_3N_4 + SiC + NaF + 2H_2,\end{aligned} \tag{3}$$

$$\begin{aligned}&5Si + 2C + NaN_3 + NH_4F \\ &= Si_3N_4 + 2SiC + NaF + 2H_2,\end{aligned} \tag{4}$$

$$\begin{aligned}&7Si + 4C + NaN_3 + NH_4F \\ &= Si_3N_4 + 4SiC + NaF + 2H_2,\end{aligned} \tag{5}$$

$$\begin{aligned}&7Si + C + 2NaN_3 + 2NH_4F \\ &= 2Si_3N_4 + SiC + 2NaF + 2H_2,\end{aligned} \tag{6}$$

$$\begin{aligned}&13Si + C + 4NaN_3 + 4NH_4F \\ &= 4Si_3N_4 + SiC + 4NaF + 2H_2.\end{aligned} \tag{7}$$

In these equations, the composition of the reaction products is expressed in moles; when passing to wt %, the following ratios are obtained for the theoretical composition of the target compositions Si_3N_4–SiC, provided that the water-soluble side salt NaF is removed from the reaction products:

(3): $Si_3N_4 + SiC = 77.8\%\ Si_3N_4 + 22.2\%\ SiC$,

(4): $Si_3N_4 + 2SiC = 63.6\%\ Si_3N_4 + 36.4\%\ SiC$,

(5): $Si_3N_4 + 4SiC = 46.7\%\ Si_3N_4 + 53.3\%\ SiC$,

(6): $2Si_3N_4 + SiC = 87.5\%\ Si_3N_4 + 12.5\%\ SiC$,

(7): $4Si_3N_4 + SiC = 93.3\%\ Si_3N_4 + 6.7\%\ SiC$.

For the experimental study, as the initial raw materials we used (hereinafter, wt %) silicon powder of the "Kr0" grade (content of the main substance ≥98.8%, $d_{0.5}$ = 5 μm), ammonium fluoride powder of the pure grade, (≥99.1%, 20 μm), sodium azide powder of the pure grade (≥98.71%, 100 μm), and technical carbon of the "P701" grade (≥88.0%, 70 nm in the form of agglomerates up to 1 μm) (Russian State Standards). A mixture of dried initial powders, taken in a given ratio, was manually mixed in a porcelain mortar for 5–10 min until visually uniform distribution of the components. The prepared mixture of powders (charge) was poured into a tracing glass with a diameter of 30 mm and a height of 45 mm, placed in a filter assembly made of carbon cloth, and two tungsten-rhenium thermocouples were inserted. The bulk relative density of the powder mixtures averaged 40% of the maximum possible density of the non-porous mixtures of the given compositions. The assembled construction was installed on the object shelf of a constant pressure SHS-Az laboratory reactor with a working volume of 4.5 L [26]. A nitrogen gas pressure of 4 MPa was created in the reactor and combustion was initiated with an electric tungsten filament.

After synthesis, the sample was removed from the reactor and manually disintegrated to a free-flowing powdery state in a porcelain mortar. Then, the powdery combustion product was washed with distilled water from the residual by-product, sodium fluoride, to achieve the acid-base balance of the wash water pH 8.

The elemental and phase composition, microstructure and particle size of combustion products were investigated. The phase composition of the synthesized products was determined on an ARL E'trA-138 powder X-ray diffractometer equipped with an X-ray tube with a copper anode with a maximum power of 2200 W. Scanning was performed in the 2θ range of angles (20°–80°) at a speed of 2 deg/min. The interpretation of the diffraction patterns and the quantitative assessment of the phase composition by the Rietveld method were performed in the PDXL 1.8 software using the PDF-2009 and COD-2019 crystallographic databases. The morphology and particle size of the synthesized compositions were studied using images of the microstructure of combustion products on a Jeol JSM-6390A scanning electron microscope.

RESULTS

The results of the experimental determination of the combustion parameters, namely, the maximum temperature T_c, the rate U_c, the maximum pressure p_m, the theoretical (M_t) and practical (M_{pr}) yield of condensed combustion products of charge compositions for the synthesis of ceramic nitride-carbide compositions Si_3N_4–SiC are presented in Table 1.

From the analysis of the data given in Table 1, it follows that an increase in the amount of silicon in the charge with the same amount of carbon, i.e. an increase in the proportion of silicon nitride in the product leads to an increase in the temperature and combustion rate, and an increase in the proportion of silicon carbide in the product with an increase in the amount of carbon in the charge leads to a decrease in the temperature and combustion rate. It can be seen that the practical yield of the product is quite close to the theoretical one, the difference is from 2.8 to 8.5%, and it is the greater, the higher the content of NH_4F salt in the charge.

Table 1. Combustion parameters of charge compositions for synthesis Si_3N_4–SiC

Composition of the charge compositions in accordance with reactions (3)–(7)	T_c, °C	U_c, cm/s	p_m, MPa	m_{charge}, g	M_t, g	M_{pr}, g
$4Si + C + NaN_3 + NH_4F$	1955	0.80	4.69	23.21	22.80	21.87
$5Si + 2C + NaN_3 + NH_4F$	1910	0.79	4.58	23.98	23.63	22.96
$7Si + 4C + NaN_3 + NH_4F$	1902	0.76	4.53	25.08	24.79	23.18
$7Si + C + 2NaN_3 + 2NH_4F$	2098	0.83	4.81	22.73	22.29	21.34
$13Si + C + 4NaN_3 + 4NH_4F$	2225	0.85	5.03	22.46	22.01	20.13

Table 2. Composition of combustion products of charge compositions, wt %

Charge compositions in accordance with reactions (3)–(7)	α-Si_3N_4	β-Si_3N_4	α-Si_3N_4 + β-Si_3N_4	β-SiC	Si_f
$4Si + C + NaN_3 + NH_4F$ (3)	70.2	19.4	89.6	9.7	0.7
$5Si + 2C + NaN_3 + NH_4F$ (4)	50.9	19.5	70.4	23.9	5.7
$7Si + 4C + NaN_3 + NH_4F$ (5)	38.2	17.6	55.8	41.8	2.4
$7Si + C + 2NaN_3 + 2NH_4F$ (6)	68.4	27.4	95.8	3.6	0.6
$13Si + C + 4NaN_3 + 4NH_4F$ (7)	69.3	28.1	97.4	1.6	1.0

Figure 1 and Table 2 shows the X-ray diffraction patterns and the results of the quantitative X-ray powder diffraction analysis of the composition of the combustion products of the initial mixtures of powders (charge) according to reactions (3)–(7) after water washing and removal of NaF.

The washed combustion products of all the investigated charge compositions consist of four phases: silicon nitride of two modifications (α-Si_3N_4 and β-Si_3N_4), silicon carbide (β-SiC), and free silicon impurities (Si_f). Note that the presence of small impurities of unreacted silicon is also typical for other cases

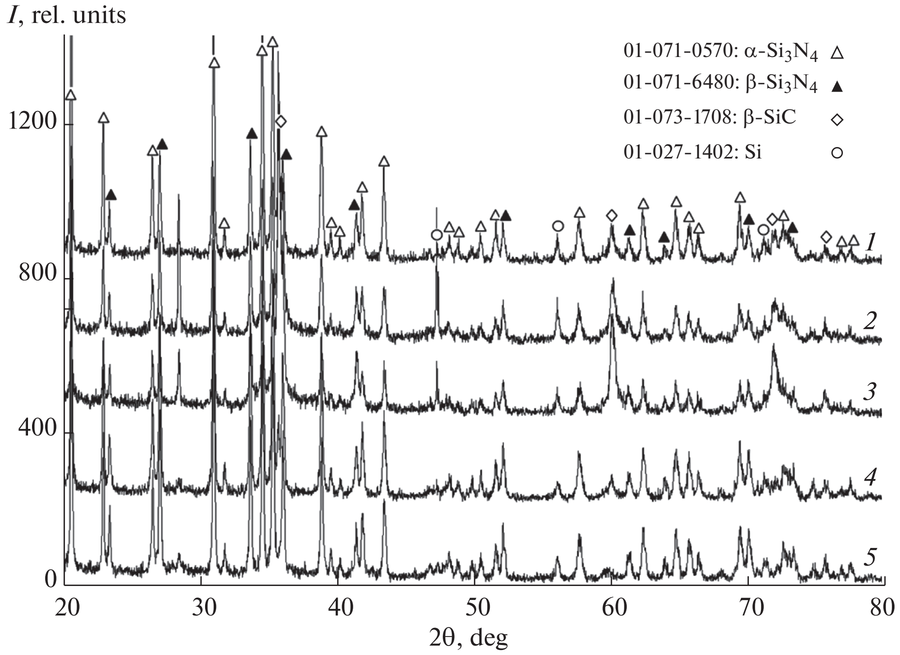

Fig. 1. X-ray diffraction patterns of combustion products of charge compositions in accordance with reactions (3)–(7): (*1*) $4Si + C + NaN_3 + NH_4F$ (3); (*2*) $5Si + 2C + NaN_3 + NH_4F$ (4); (*3*) $7Si + 4C + NaN_3 + NH_4F$ (5); (*4*) $7Si + C + 2NaN_3 + 2NH_4F$ (6); (*5*) $13Si + C + 4NaN_3 + 4NH_4F$ (7).

of using the combustion process to obtain a composition of Si_3N_4–SiC powders [27–29]. Other differences between the experimentally determined composition of combustion products from the calculated theoretical composition (3)–(7) are discussed below together with the microstructure of combustion products.

The experimental composition of the combustion products of reaction (3) (89.6% Si_3N_4 + 9.7% SiC + 0.7% Si_f) differs from the theoretical composition (3) (77.8% Si_3N_4 + 22.2% SiC) by a significantly higher content of silicon nitride, almost half the content of carbide silicon, and the presence of a small impurity Si_f. In this case, silicon nitride consists mainly of the α-Si_3N_4 modification, the content of which is four times higher than the content of β-Si_3N_4. The microstructure of the combustion products present Fig. 2 shows fibers with a diameter of 150–500 nm and a length of up to 5 μm, typical of α-Si_3N_4, as well as particles of an equiaxed form of silicon carbide, which are in the form of both individual particles and agglomerates.

Thus, combustion of a mixture of the initial powders of reaction (3) makes it possible to obtain a composition of submicron powders close to the composition Si_3N_4–10% SiC, with a predominant content of α-Si_3N_4 and a small content of free silicon impurities (0.7%).

In the case of reaction (4), with an increase in the charge of silicon from 4 to 5 moles and carbon from 1 to 2 moles in comparison with the charge of reaction (3), in the combustion products of the charge of reaction (4) (Table 2), a reduced content of α-modification of silicon nitride with an increased content of silicon carbide and free silicon phases is observed: α-Si_3N_4, 50.9%; β-Si_3N_4, 19.5%; SiC, 23.9%; Si_f, 5.7%. Here, the content of α-Si_3N_4 fibers should be ~50% of the volume of the powder mixture, but Fig. 2 shows a significantly lower content of single fibers with a diameter of 100–250 nm with a predominant content of equiaxed particles with a size of 100–500 nm in the form of individual particles and agglomerates, which indicates the formation of a significant part of α-Si_3N_4 (along with β-Si_3N_4 and Si_f) in the form particles of an equiaxed shape with an increased carbon content in the charge. The conclusion about the effect of the increased carbon content rather than silicon is explained by the fact that the silicon content in the charge of reaction (4) increased by only 25% in comparison with the charge of reaction (3), and the carbon content increased by 100%, as well as that with the same carbon content (1 mol) but an increased silicon content (7 mol) in the charge of reaction (6) and 13 moles in the charge of reaction (7), α-Si_3N_4 is formed mainly in the form of fibers.

In general, the composition of the synthesized ultradispersed powder composition 70.4% Si_3N_4 + 23.9% SiC + 5.7% Si_f differs from the theoretical composition (4) 63.6% Si_3N_4 + 36.4% SiC by a smaller difference in the content of silicon nitride and silicon carbide, but a significantly higher content of Si_f impurity than in the case of reaction (3).

The results of X-ray powder diffraction analysis of the combustion products of the charge of reaction (5) 7Si + 4C + NaN_3 + NH_4F presented in Table 2 show that with an increase in the carbon content by four times and the silicon content by a factor of two in comparison with the charge of reaction (3), the combustion products of the charge (5) contain significantly lower amount of nitride silicon and higher amount silicon carbide: α-Si_3N_4, 38.2%; β-Si_3N_4, 17.6%; SiC, 41.8%; Si_f, 2.4%. In addition, this composition differs from the theoretical composition (5) 46.7% Si_3N_4 + 53.3% SiC with respect to α-Si_3N_4 and SiC while maintaining the content of β-Si_3N_4. A comparison of the microstructures shows that the combustion products also consist mainly of particles of an equiaxed shape, but differ greatly in size. In the case of reaction (5) with a high content of silicon and carbon in the charge, they are a mixture of silicon nitride and silicon carbide in the form of submicron particles 150–500 nm in size and much larger particles up to 2 μm in size.

It follows from Table 2 that as a result of the combustion of the charge of reaction (6), which contains twice as much silicon as compared to the charge of reaction (3) at the same carbon content, approximately the same amount of α-Si_3N_4 is formed and almost 20% more β-Si_3N_4, almost three times less silicon carbide and almost the same amount of free silicon impurity: α-Si_3N_4, 68.4%; β-Si_3N_4, 27.4%; SiC, 3.6%; Si_f, 0.6%. The composition of the synthesized composition differs from the theoretical composition (6) 87.5% Si_3N_4 + 12.5% SiC by a noticeably higher content of silicon nitride and a significantly lower (almost four times) content of silicon carbide. According to Fig. 2, mainly typical for α-Si_3N_4 fibers with a diameter of 100–250 nm and a length of up to 3 μm and equiaxed particles with a size of 100–500 nm in the form of individual particles and agglomerates are formed.

In the case of the mixture of reaction (7) with a much higher content of silicon, sodium azide, and ammonium fluoride as compared to the mixture (3) with the same carbon content, the following composition of the synthesized composition was obtained (Table 2): α-Si_3N_4, 69.3%, β-Si_3N_4, 28.1%, SiC, 1.6%, Si_f, 1.0%, which differs from the composition according to reaction (6) only by an even lower silicon carbide content, which is four times less than the theoretical one (7): 93.3% Si_3N_4 + 6.7% SiC. According to Fig. 2, as in the previous case, the combustion products are mainly fibers with a diameter of 100–250 nm and a length of up to 3 μm and equiaxed particles with a size of 100–500 nm in the form of individual particles and agglomerates.

(a) Reaction (3) $4Si + C + NaN_3 + NH_4F$ (b)

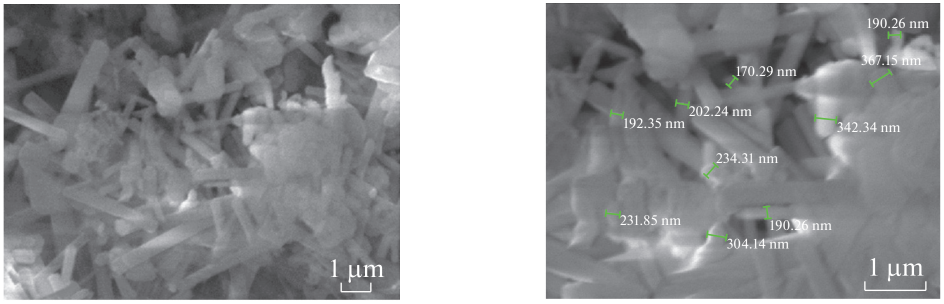

Reaction (4) $5Si + 2C + NaN_3 + NH_4F$

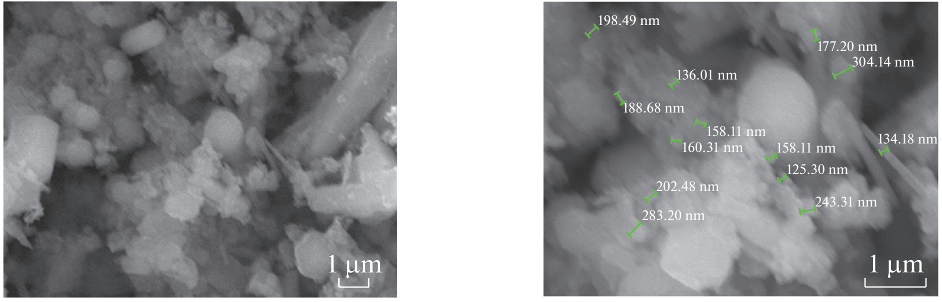

Reaction (5) $7Si + 4C + NaN_3 + NH_4F$

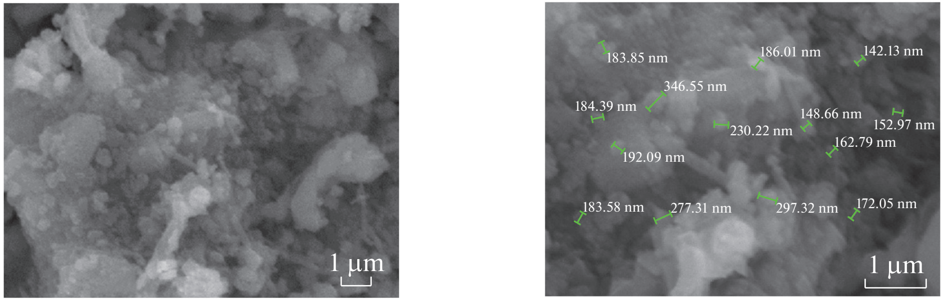

Reaction (6) $7Si + C + 2NaN_3 + 2NH_4F$

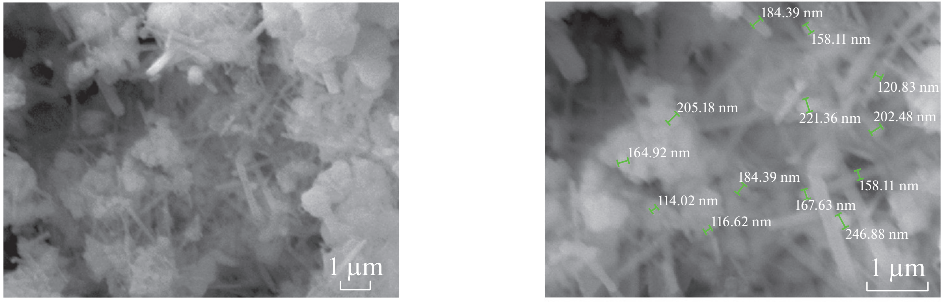

Reaction (7) $13Si + C + 4NaN_3 + 4NH_4F$

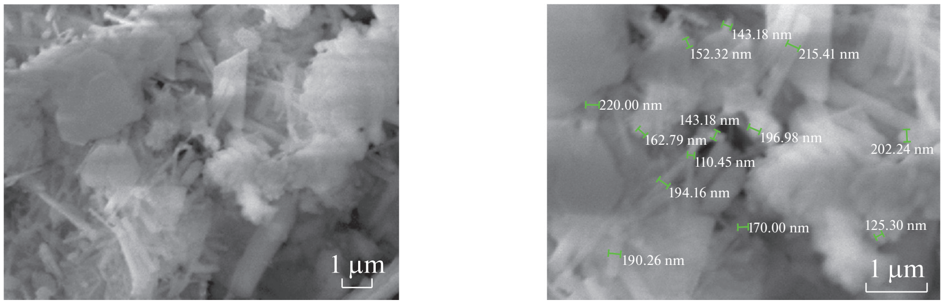

Fig. 2. Microstructure of the combustion products of the mixture of reactions (3)–(7) at a magnification of (a) ×10000 and (b) ×20000.

DISCUSSION

When implementing the azide SHS process to obtain a highly dispersed composition of Si_3N_4–SiC powders, the experimental composition noticeably differs from the calculated theoretical composition, primarily in the significantly lower content of silicon carbide. Figure 3 shows the dependence of the experimentally found silicon carbide content SiC_e on the theoretical content SiC_t plotted from the results of Table 2 and Eqs. (3)–(7).

Such a difference between the experimental and theoretical results can be explained by the peculiarities of the formation of silicon carbide when obtaining a composition of Si_3N_4–SiC powders by burning a mixture of silicon and carbon powders in a nitrogen atmosphere [27–29]. The reaction for the synthesis of silicon carbide from elemental powders Si + C = SiC has a small thermal effect (73 kJ/mol) and cannot provide a self-propagating combustion mode, while the reaction for the synthesis of silicon nitride from silicon powder in gaseous nitrogen $3Si + 2N_2 = Si_3N_4$ is highly exothermic with a thermal effect of 756 kJ/mol and can proceed in combustion mode. Therefore, when the combustion of a mixture of silicon and carbon powders is initiated, silicon nitride is first synthesized with an increase in temperature to high values exceeding 2273 K, at which the synthesized Si_3N_4 dissociates, and then the resulting silicon reacts with carbon, forming SiC, which is more stable at high temperatures. The formation of SiC proceeds until the complete consumption of carbon, and the remaining unused silicon turns into Si_3N_4. In the case of combustion of charge compositions of reactions (3)–(7), more silicon nitride and less silicon carbide are formed than should be according to reactions (3)–(7), but free carbon is not found in the combustion products. The reason may be that a part of very small particles of technical carbon (soot) is removed (blown out) from the burning highly porous charge sample by gases released during combustion and does not participate in the conversion of Si_3N_4 to SiC. As a result, more silicon nitride and less silicon carbide remain in the combustion products than should be according to reaction (3)–(7). The lower the carbon content in the charge in comparison with the silicon content in these equations, the higher the combustion temperature and the greater the gas release, the greater the relative carbon loss due to gas removal, and the more SiC_e differs from SiC_t. It should be noted that the above approximation dependence $SiC_e(SiC_t)$ makes it possible to predict the actual composition of the synthesized composition of Si_3N_4–SiC powders using reaction equations of the type (3)–(7) under the considered experimental conditions. To approximate the calculated composition of the synthesized Si_3N_4–SiC composition, it is necessary to carry out further studies with possible technological changes, namely using an excess of carbon powder, changing such parameters as the pressure of gaseous nitrogen in the reactor, the density and volume of the charge sample, etc.

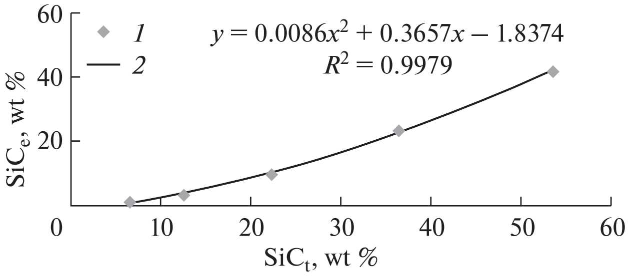

Fig. 3. Dependence of the experimental content of SiC_e on the theoretical SiC_t in the composition of powders Si_3N_4–SiC and its polynomial approximation, in which $y = SiC_e$, $x = Si_t$, R^2 is the approximation reliability value.

CONCLUSIONS

The efficiency of using the activating additive of the halide salt NH_4F for the preparation of a highly dispersed composition of Si_3N_4–SiC powders with different phase ratios in a wide range of silicon carbide content (from 1.6 to 41.8%) by the azide SHS method has been confirmed. The synthesized compositions are distinguished by a high content of α-Si_3N_4 (2.17–3.61 times more than β-Si_3N_4). With a high carbon content in the charge, leading to the synthesis of 23.9 and 41.8% silicon carbide in the composition, α-Si_3N_4 is formed mainly in the form of particles of an equiaxed rather than fibrous form. The impurity content of free silicon does not exceed 1.0% for composites with SiC contents up to 10%, but reaches 2.4–5.7% with SiC contents of 23.9 and 41.8%, which is obviously due to the high silicon content in the initial charge and the incomplete reaction of SiC formation. With a SiC content of 1.6 to 23.9%, the Si_3N_4–SiC composites are submicron and consist of fibers 100–500 nm in diameter and up to 5 μm in length, as well as equiaxed particles 100–500 nm in size in the form of individual particles and their agglomerates. At a SiC content of 41.8%, the Si_3N_4–SiC composition is a mixture of submicron particles 150–500 nm in size with much larger particles up to 2 μm in size. The obtained composite Si_3N_4–SiC powders differ from those synthesized earlier using the combustion process both in a higher dispersion and a higher content of α-Si_3N_4, and therefore they are promising for use in the manufacture of composite ceramic materials with improved properties at lower sintering temperatures. However, for this, it is necessary to refine the process of azide SHS of the composition of highly dispersed Si_3N_4–SiC powders with respect to technological changes in order to approximate the calculated composition and reduce the content of free silicon in it.

FUNDING

The study was supported by the Russian Foundation for Basic Research, project no. 20-38-90158.

CONFLICT OF INTEREST

The authors declare that they have no conflicts of interest.

REFERENCES

1. T. Ya. Kosolapova, T. V. Andreeva, T. B. Bartnitskaya, et al., *Non-Metallic Refractory Compounds* (Metallurgiya, Moscow, 1985) [in Russian].
2. R. A. Andrievskii and I. I. Spivak, *Silicon Nitride and Materials Based on It* (Metallurgiya, Moscow, 1984) [in Russian].
3. O. A. Ageev, A. E. Belyaev, N. S. Boltovets, et al., *Silicon Carbide: Technology, Properties, Application* (ISMA, Khar'kov, 2010) [in Russian].
4. B. B. Bobovich, *Non-Metallic Construction Materials* (MGIU, Moscow, 2009).
5. B. Basu and K. Balani, *Advanced Structural Ceramics* (John Wiley & Sons Inc, Hoboken, New Jersey, 2011).
6. E. P. Simonenko, N. P. Simonenko, V. A. Nikolaev, et al., Russ. J. Inorg. Chem. **64**, 1456 (2019). https://doi.org/10.1134/S0036023619110202
7. E. P. Simonenko, N. P. Simonenko, V. G. Sevastyanov, and N. T. Kuznetsov, Russ. J. Inorg. Chem. **64**, 1697 (2019). https://doi.org/10.1134/S0036023619140079
8. E. P. Simonenko, N. P. Simonenko, A. N. Gordeev, et al., Russ. J. Inorg. Chem. **65**, 606 (2020). https://doi.org/10.1134/S0036023620040191
9. N. P. Shapkin, E. K. Papynov, O. O. Shichalin, et al., Russ. J. Inorg. Chem. **66**, 629 (2021). https://doi.org/10.1134/S0036023621050168
10. Yu. L. Pilipovskii, T. V. Grudina, A. B. Sapozhnikova, et al., *Composite Materials in Mechanical Engineering* (Tekhnika, Kiev, 1990) [in Russian].
11. K. Niihara, K. Izaki, and T. Kawakami, J. Mater. Sci. Lett. **10**, 112 (1990).
12. K. Niihara, J. Ceram. Soc. Jpn. **99**, 974 (1991). https://doi.org/10.2109/jcersj.99.974
13. G. Pezzotti, J. Am. Ceram. Soc. **76**, 1313 (1993). https://doi.org/10.1002/chin.199330007
14. Y.-H. Koh, H.-W. Kim, and H.-E. Kim, Scrp. Mater. **44**, 2069 (2001). https://doi.org/10.1016/S1359-6462(01)00885-5
15. M. Khajelakzay and S. R. Bakhshi, Ceram. Int. **43**, 6815 (2017).
16. P. Palmero, Nanomaterials **5**, 656 (2015).
17. L. Montanaro and P. Palmero, Ceramics **2**, 296 (2019). https://doi.org/10.3390/ceramics2020024
18. I. V. Kozerozhets, G. P. Panasyuk, E. A. Semenov, et al., Russ. J. Inorg. Chem. **65**, 1943 (2020). https://doi.org/10.1134/S0036023620120086
19. T. Yanai and K. Ishizaki, J. Ceram. Soc. Jpn. **101**, 764 (1993). https://doi.org/10.2109/jcersj.101.764
20. R. Riedel, M. Seher, and G. Becker, J. Eur. Ceram. Soc. **5**, 113 (1989). https://doi.org/10.1016/0955-2219(89)90018-6
21. J. Suri, L. Shaw, and M. F. Zawrah, Int. J. Appl. Ceram. Tech. **9**, 291 (2012). https://doi.org/10.1111/j.1744-7402.2011.00710.x
22. J. Hojo, H. Meada, and A. Kato, Yogyo-Kyokai-Shi. **95**, 45 (1987).
23. H. J. Lee, K. Eguchi, and T. J. Am. Yoshida, Ceram. Soc. **73**, 3356 (1990).
24. A. P. Amosov, I. P. Borovinskaya, A. G. Merzhanov, and A. E. Sytchev, Int. J. Self-Propag. High-Temp. Synt. **14**, 165 (2005).
25. A. S. Rogachev and A. S. Mukasyan, *Combustion for Material Synthesis* (CRC Press, New York, 2014).
26. E. A. Levashov, A. S. Mukasyan, A. S. Rogachev, and D. V. Shtansky, Int. Mater. Rev. 203–218 (2016). https://doi.org/10.1080/09506608.2016.1243291
27. J. Zeng, Y. Miyamoto, and O. Yamada, J. Am. Ceram. Soc. **74**, 2197 (1989).
28. D. Kata, J. Lis, R. Pampuch, and L. Stobierski, Int. J. Self-Propag. High-Temp. Synt. **7**, 475 (1998).
29. G. L. Khachatryan, A. B. Arutyunyan, and S. L. Kharatyan, Comb. Expl. Shock Waves **42**, 543 (2006).
30. A. P. Amosov and G. V. Bichurov, *Azide Technology of Self-Propagating High-Temperature Synthesis of Micro- and Nanopowders of Nitrides* (Mashinostroenie-1, Moscow, 2007) [in Russian].
31. G. V. Bichurov, L. A. Shiganova, and Yu. V. Titova, *Azide Technology of Self-Propagating High-Temperature Synthesis of Micro- and Nanopowders of Nitride Compositions* (Mashinostroenie, Moscow, 2012) [in Russian].
32. Y. V. Titova, A. P. Amosov, and A. A. Ermoshkin, et al., Russ. J. Non-Ferr. Met. **55**, 620 (2014).
33. G. V. Bichurov, *Nitride Ceramics: Combustion Synthesis, Properties, and Applications*, Ed. by A. A. Gromov and L. N. Chukhlomina (Wiley-VCH, Weinheim, 2015).
34. Y.-J. Lee, D.-Y. Kim, K.-H. Lee, et al., Nanoscale Res. Lett. **8**, 126 (2013). https://doi.org/10.1186/1556-276X-8-126
35. H. H. Nersisyan, J. H. Lee, J.-R. Ding, et al., Progr. Energy Comb. Sci. **63**, 79 (2017). https://doi.org/10.1016/j.pecs.2017.07.0020360-1285

Translated by V. Avdeeva